Characteristics and variability of storm tracks in the north Pacific, Bering Sea, and Alaska

Article

Published Version

Characteristics and Variability of Storm Tracks in the North Pacific, Bering Sea, and Alaska*

MICHEL D. S. MESQUITA

Department of Atmospheric Sciences, and International Arctic Research Center, University of Alaska Fairbanks, Fairbanks, Alaska, and Bjerknes Centre for Climate Research, Bergen, Norway

DAVID E. ATKINSON

Department of Atmospheric Sciences, and International Arctic Research Center, University of Alaska Fairbanks, Fairbanks, Alaska

KEVIN I. HODGES

National Centre for Earth Observation, University of Reading, Reading, United Kingdom

(Manuscript received 7 January 2009, in final form 7 June 2009)

ABSTRACT

The North Pacific and Bering Sea regions represent loci of cyclogenesis and storm track activity. In this paper climatological properties of extratropical storms in the North Pacific/Bering Sea are presented based upon aggregate statistics of individual storm tracks calculated by means of a feature-tracking algorithm run using NCEP–NCAR reanalysis data from 1948/49 to 2008, provided by the NOAA/Earth System Research Laboratory and the Cooperative Institute for Research in Environmental Sciences, Climate Diagnostics Center. Storm identification is based on the 850-hPa relative vorticity field (ζ) instead of the often-used mean sea level pressure; ζ is a prognostic field, a good indicator of synoptic-scale dynamics, and is directly related to the wind speed. Emphasis extends beyond winter to provide detailed consideration of all seasons.

Results show that the interseasonal variability is not as large during the spring and autumn seasons. Most of the storm variables—genesis, intensity, track density—exhibited a maxima pattern that was oriented along a zonal axis. From season to season this axis underwent a north–south shift and, in some cases, a rotation to the northeast. This was determined to be a result of zonal heating variations and midtropospheric moisture patterns. Barotropic processes have an influence in shaping the downstream end of storm tracks and, together with the blocking influence of the coastal orography of northwest North America, result in high lysis concentrations, effectively making the Gulf of Alaska the ''graveyard'' of Pacific storms. Summer storms tended to be longest in duration. Temporal trends tended to be weak over the study area. SST did not emerge as a major cyclogenesis control in the Gulf of Alaska.

1. Introduction

The coast of Alaska is experiencing serious impacts owing to erosion and inundation. The primary drivers are waves and surge generated by strong winds that are typically associated with storms. Understanding the trends and dynamics of coastal erosion in Alaska is grounded in grasping both the dynamics and the climatology of storms in the North Pacific (NP) and Bering Sea and how they vary spatially and temporally (Atkinson 2005; Rachold et al. 2005). This issue extends beyond the physical processes of erosion—environmental and societal impacts are equally severe (Graham and Diaz 2001)—and includes the maritime industries (fishing, shipping) and subsistence hunting activities. The motivation to improve regional-scale understanding of storm track dynamics and patterns is thus strong. Storms are also a means by which the atmosphere redresses sinks

* Bjerknes Centre for Climate Research Publication Number A 248.

Corresponding author address: Michel dos Santos Mesquita, Allegaten 55, Bjerknes Centre for Climate Research, NO-5007, Bergen, Norway.
E-mail: michel.mesquita@bjerknes.uib.no

DOI: 10.1175/2009JCLI3019.1

and sources of energy and momentum; analyses with these theoretical meteorological objectives in mind are important for aiding our understanding of large-scale climate dynamics (Murray and Simmonds 1991).

Various analyses of storm activity have appeared in the literature; most have focused on the Northern Hemisphere as a whole, with the Arctic being separately targeted in some instances (Hoskins and Hodges 2002; Keegan 1958; McCabe et al. 2001; Serreze 1995; Sorteberg and Walsh 2008; Whittaker and Horn 1984; Zhang et al. 2004). Relatively few, however, have focused specifically on the North Pacific and Bering Sea regions (Graham and Diaz 2001; Norris 2000) apart from identifying the prominent North Pacific storm track. Less common still are studies that consider seasons other than winter: a summer discussion is unusual and autumn/spring, the equinoctial seasons, are almost never explicitly considered. Autumn is examined in Key and Chan (1999); however, they do not explicitly focus on the North Pacific.

Trends in storm activity have been examined in several papers. McCabe et al. (2001), using Serreze's sea level pressure (SLP)-based algorithm and National Centers for Environmental Prediction–National Center for Atmospheric Research (NCEP–NCAR) reanalysis data, studied storm track trends in the Northern Hemisphere for the period 1959–97. They found an increase in high-latitude winter cyclone frequency and a decrease in midlatitude winter cyclone frequency over this period. Graham and Diaz (2001), using NCEP–NCAR reanalysis data and their own algorithm also based on SLP, calculated trends in the NP (defined only as far north as 50°N) and found an overall winter [December–February (DJF)] cyclone frequency trend of 0.21 cyclones per year over the period 1948–98. Key and Chan (1999), using NCEP–NCAR reanalysis data, studied storm tracks using the tracking algorithm of Bell and Bosart (1989), which is based on the geopotential height at two levels (1000 and 500 mb). Interestingly, even as far back as 1989, they found that the surface cyclone frequency in the Arctic had increased during all seasons [DJF, March–May (MAM), June–August (JJA), and September–November (SON)], while surface cyclone frequency in the midlatitudes had decreased in both the NH and SH. They also found opposite signs in trends at 1000 and 500 mb, which could indicate that the systems had become shallower.

Storm activity analyses are generally derived from climatologies that are developed by establishing a definition of a ''storm,'' accumulating counts of their occurrences, and extracting statistics to determine their climatological characteristics (e.g., wind speed, ground speed, and duration). Analyses of storm activity, such as reviewed above, have used different methods to diagnose the storms, which vary in perspective (Lagrangian, Eulerian), method (manual and/or automated tracking), variable (mean sea level pressure, geopotential height, relative vorticity, quasigeostrophic vorticity, etc.), and tracking method (finding the central pressure in an MSLP field, finding the maxima in the relative vorticity field, and/or finding the storm center by analyzing satellite imagery). Considering studies that have included the North Pacific the following range of approaches may be noted: Graham and Diaz (2001) used their algorithm based on SLP from a Lagrangian perspective; Norris (2000) used the root-mean-squared daily vertical velocity at 500 mb during the summer season to diagnose storm tracks in the NP; and Simmonds and Keay (2002) used the Melbourne University cyclone finding and tracking scheme (Murray and Simmonds 1991) based on the geostrophic vorticity computed from the MSLP.

The key starting point in any analysis of storm activity is the event-level definition of a storm. The most common meteorological variable used for this purpose has been mean SLP (MSLP), implemented in manual (Pickart et al. 2009; Whittaker and Horn 1984) and various automated tracking schemes (Murray and Simmonds 1991; Serreze et al. 1997; Zhang et al. 2004). Another meteorological variable that has been used is relative vorticity (ζ). Sinclair (1994), using the method of Murray and Simmonds (1991), makes an important point about the poleward displacement of the pressure minimum relative to the vorticity maxima in the presence of a background zonal wind field, which is an advantage of the method. In particular, the method defined by Hodges (1994, 1995, 1996, 1999) has also been found to yield satisfactory results for several reasons (Barry and Carleton 2001; Hoskins and Hodges 2002). First, contrasted with MSLP-based approaches, relative vorticity is more sensitive to small, rapidly moving systems because MSLP tends to preferentially identify larger, slower-moving systems. In a geostrophic sense, vorticity focuses more on the small spatial scale end of the synoptic range so that more systems are identified than by using MSLP, for example, which focuses more on the large-scale end (Hodges et al. 2003). This is important for high-latitude work where small-scale features can occur with greater frequency than in the midlatitudes (Twitchel et al. 1989).

Second, MSLP can be adversely influenced by the background as discussed by Sinclair (1994). Also, a low pressure center situated within a larger region of low pressure can possess a weak pressure gradient which means surface winds are weak (Fig. 1). An algorithm based on identifying pressure minima would identify and categorize the system as strong due to a low absolute pressure reading (e.g., 956 mb in Fig. 1); however, the pressure gradient in the vicinity of the low pressure center

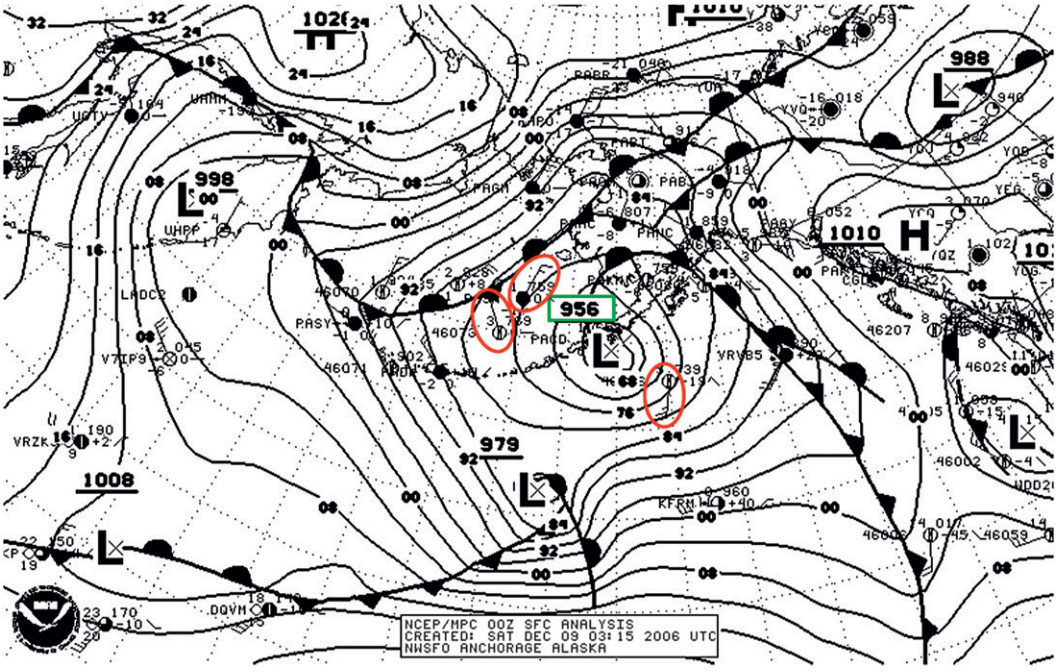

FIG. 1. Mean sea level pressure plot showing a low pressure system over the eastern Aleutian Islands on 9 Dec 2006. The central pressure is 956 mb (green box). Despite the deep central pressure the surface observed winds are weak (red ellipsis), on the order of 15 kt. Figure from the NCEP/Marine Prediction Center 0000 UTC surface analysis, provided by the NOAA/NWS Forecast Office, Anchorage, Alaska.

is not very strong. Third, the presence of relative vorticity (ζ) is an important mechanism in the initiation of extratropical storms. Its use thus enables identification of a storm earlier in its life cycle (Sorteberg and Walsh 2008), which can aid the understanding of genesis dynamics. Fourth, ζ is important to the dynamical maintenance and growth of a system, so its use also facilitates ongoing system monitoring. Finally, relative vorticity is also related directly to wind speed because its derivation is simply the vertical component of the curl of the relative velocity, that is,

$$\zeta \equiv \mathbf{k} \cdot (\nabla \times \mathbf{U}) = \frac{\partial v}{\partial x} - \frac{\partial u}{\partial y}. \quad (1)$$

Linking storm track information results directly to winds also improves their utility for secondary studies (e.g., coastal erosion) that depend upon wind forcing. For these reasons, therefore, storm climatology results based on Hodges' algorithm form the bases of the analyses presented here.

An important point that has often been overlooked in storm climatology analyses, especially with regards to impacts in northerly latitudes, is autumn activity. Autumn is an important time of year in the Arctic because it is the time of least ice, and therefore greatest open water exposure (see Fig. 12, where the 0° isotherm provides a functional indication of the average sea ice extent). In the region of study for this paper, autumn is also a time when the jet stream position and the occurrence of remnant tropical cyclone activity can create a particularly strong storm response.

Thus, it is the objective of this paper to aggregate storm activity results for the North Pacific and Bering Sea regions obtained using a robust and proven storm tracking algorithm, focusing on the seasonal time frame, including autumn. It also explores trends in storm activity responses, including trend considerations of the pre- and post-1979 periods and discussions of changes in SST. Changes in horizontal gradients of SST affect baroclinic instability, which in turn influences storm tracks. The seasonal climate over the Pacific has also undergone changes in the mid to late 1970s (Graham and Diaz 2001). These analyses will be conducted via a thorough discussion of different track variables, making this effort one of the most complete and updated studies of storm tracks for the North Pacific/Bering Sea.

Hence, the present paper is aimed at describing and understanding the climatology and trends of the storms in the North Pacific region, including the Bering Sea and the Gulf of Alaska, for standard climatological seasons, that is, winter (DJF), spring (MAM), summer (JJA), and autumn (SON). The following questions will be addressed:

- Has there been a relative change in the seasonal patterns of storminess in these regions?
- What are the characteristics of equinoctial season storms? (This question is important since spring and autumn are not typically addressed, yet many of the most problematic storms in the Alaska region occur in the autumn.)
- What is the ground track speed of storms? (The threat presented by a storm is increased if it is slow moving. Knowing how fast systems move is an important objective.)

Section 2 discusses the methodology used; section 3 presents the results, focusing on a seasonal intercomparison of the climatologies and then on a discussion of the trends in the tracking variables; finally, even though a direct comparison with magnitudes from other climatologies is not immediately possible given the different normalizations in other studies (Simmonds and Keay 2002), a discussion will conclude the paper that places these results in light of the existing literature, whenever possible. Owing to space constraints, detailed consideration of these patterns in the context of other major circulation mode indices will be considered in another paper.

2. Methodology

Storm systems were identified and tracked using the algorithm developed by Hodges (1994, 1995, 1996, 1999), and run for the NH and subset for this study. In this algorithm relative vorticity is analyzed directly on the unit sphere, not a preprojected or unprojected Cartesian grid. This approach ''reduces the likelihood of introducing bias into the tracking and statistics and makes the parameters required for the tracking and statistical estimation independent of any projection'' (Hodges et al. 2003). Essentially, using a gridded dataset as input, the algorithm identifies a storm center to be a relative vorticity maximum that exceeds 1×10^{-5} s^{-1}. To solve the correspondence between the feature points in consecutive time steps, which Hodges identifies as the most difficult aspect of any storm tracking system, a specialized cost function is applied (Hodges 1995). Minimization of the cost function results in the smoothest set of tracks subject to constraints on displacement distance and the track smoothness.

Relative vorticity at 850 hPa is used as the analysis variable since 850 hPa represents a good tropospheric weather activity level for storm tracking (Hodges et al. 2003). Likewise, vorticity represents a good analysis variable because it does not depend on any extrapolation techniques, as does MSLP. The tracks have been filtered to retain only those that last longer than 2 days and travel farther than 1000 km (mobile storms).

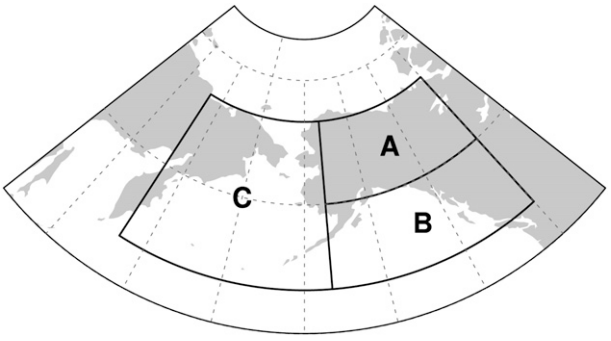

FIG. 2. Three regions in Alaska studied in this paper: (A) Alaska interior/Yukon (60°–70°N, 160°–120°W); (B) Gulf of Alaska (50°–60°N, 160°–120°W); and (C) Bering Sea (50°–70°N, 160°E–160°W).

The algorithm input data, four times daily u and v for the relative vorticity calculation, were drawn from the NCEP–NCAR Global Reanalysis 1 (GR-1) (Kalnay et al. 1996; Kistler et al. 2001) from 1948/49 to 2008, provided by NOAA/National Weather Service (NWS)/NCEP [NCEP–NCAR reanalysis data provided by the NOAA/Office of Oceanic and Atmospheric Research (OAR)/Earth System Research Laboratory (ESRL)/Physical Sciences Division (PSD), Boulder, Colorado, from their Web site at http://www.cdc.noaa.gov/]. SST data were provided by the NCEP–NCAR reanalysis as well.

Six sets of spatial statistics derived from the tracking were retained for analysis:

(i) genesis density (gdens): indicates the areas where the storm tracks start [units: number density of starting points $(10^6$ km^2 season$)^{-1}$];
(ii) track density (tdens): number density of storm tracks passing through a region per season [units: storms $(10^6$ km^2 season$)^{-1}$];
(iii) lysis density (ldens): indicates the areas where the storm tracks die out per season [units: number density of ending points $(10^6$ km^2 season$)^{-1}$];
(iv) mean intensity (int): intensity of the vortex [units: intensity in 10^{-5} s^{-1}];
(v) mean lifetime (lft): number of days the low pressure systems lasted that pass through a region;
(vi) mean speed (mspd): mean track speed (m s^{-1}).

Two major analyses were conducted on each of these variables. First, a general pattern analysis by season was conducted for the six tracking statistics. Second, assessment of trends using least squares fitting for selected variables was performed for three collective regions in and around Alaska (Fig. 2). Statistical significance was based on a t test of the linear regression coefficients. The regions studied were:

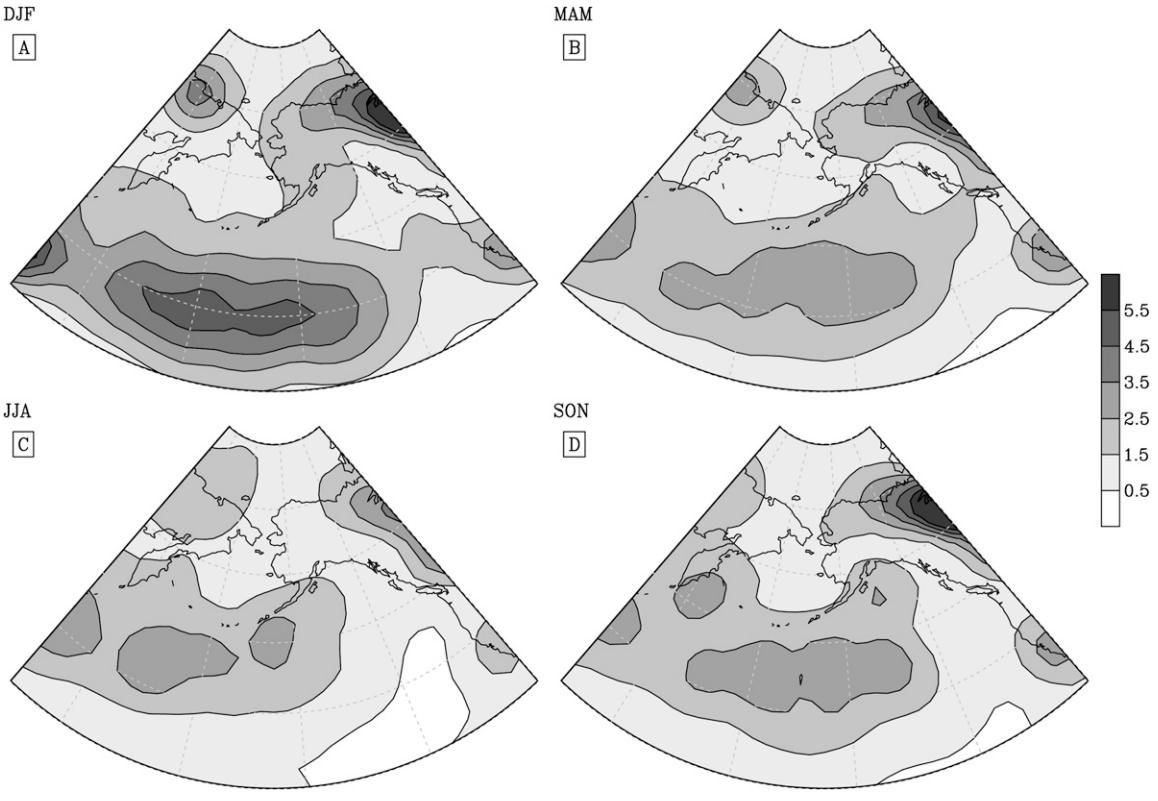

FIG. 3. Genesis density climatology in the North Pacific from 1948/49 to 2008 for the (a) winter (DJF), (b) spring (MAM), (c) summer (JJA), and (d) autumn (SON) seasons. Units: density of starting points $(10^6 \text{ km}^2 \text{ season})^{-1}$.

(i) Alaska interior/Yukon (AIY) from 60° to 70°N, 160° to 120°W;
(ii) Gulf of Alaska (GOA) from 50° to 60°N, 160° to 120°W;
(iii) Bering Sea (BeS) from 50° to 70°N, 160°E to 160°W.

The next section will discuss the main results of these analyses.

3. Results

a. Climatology

The overall pattern in the cyclogenesis density plots (Figs. 3a–d) show two major storm initiation maxima: the North Pacific and the North American continental interior. The North Pacific maximum, oriented east–west, is situated in response to the zone of strong baroclinicity that arises from a strong and persistent poleward temperature gradient. This maximum is referred to as ''secondary cyclogenesis'' in Hoskins and Hodges (2002). The strong formation area over the North American continental interior is largely a result of lee cyclogenesis behind the coastal mountain ranges, that is, cyclogenesis initiated by the conservation of potential vorticity (Holton 2004). It has been suggested that the formation area over the northern continent is also associated with land–sea temperature contrast (Serreze et al. 2001). The largest values of cyclogenesis are found in the regions bounded by 35°–45°N, 160°E–150°W over the central North Pacific and over northwestern Canada during winter; spatial patterns in other seasons are generally similar with a reduction in cyclogenesis magnitude. Generally, the Pacific track parallels lines of latitude. The maxima axes shift north and south with the seasons—farthest south (north) in winter (summer). In summer there is a distinct departure from the linear east–west pattern with the appearance of a west-northwest tending kink, or dogleg, in the axis such that the axis shifts and rotates to run roughly parallel to the eastern half of the Aleutian Islands. This is also evident to a weaker extent as a component of the autumn axis pattern.

Over Alaska, the cyclogenesis density is greatest in winter, becoming more confined to the central/northern part of Alaska during the other seasons. A similar reduction is observed over a small cyclogenesis zone over the Chukotka north coast. By summer, the cyclogenesis is present at low magnitudes over Alaska and Chukotka, with the lee cyclogenesis zone persisting east of the Canadian Rockies. Overall, the summer is the season of

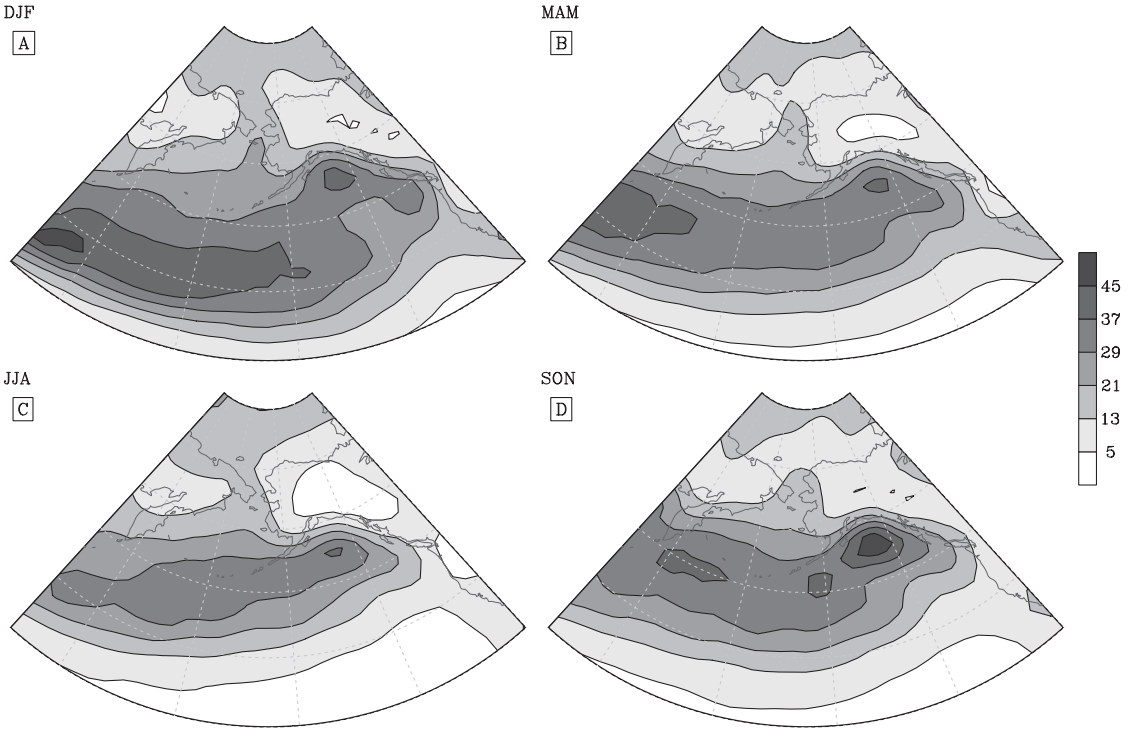

FIG. 4. As in Fig. 3 but for track density climatology. Units: storms $(10^6 \text{ km}^2 \text{ season})^{-1}$.

lowest cyclogenesis activity over the study area. The autumn cyclogenesis pattern is similar to that in spring, with the exception of extensions of the Pacific genesis zone into both the Kamchatka Peninsula/Sea of Okhotsk area and well up into the Gulf of Alaska. These extension features are unique to autumn.

The overall track density pattern (Figs. 4a–d) indicates a favored pathway running east–west in the North Pacific. A persistent collection zone in the Gulf of Alaska was also present in all seasons. Overall, track densities are highest in winter peaking at 37–45 storms $(10^6 \text{ km}^2 \text{ season})^{-1}$, although autumn has a similar magnitude peak, and lowest in summer peaking at 13–29 storms $(10^6 \text{ km}^2 \text{ season})^{-1}$. During winter, the zone of storm frequency maxima covers most of the North Pacific and the Gulf of Alaska. Spring and autumn track densities have characteristics similar to one another: both have a similar core within the broader Pacific maximum stretching over the North Pacific toward the Gulf of Alaska with a peak density exceeding 37 storms $(10^6 \text{ km}^2 \text{ season})^{-1}$. The seasonal north/south shift in the maxima axis, observed for gdens, is observed again here. In summer the storm track lies along a more northerly position, closer to the Aleutian Islands. The dogleg feature observed in genesis density was observed again for track density—most prominently in the winter, then less so in fall and spring, and finally not apparent in the summer. Spring and autumn count maxima exceeding 37 storms $(10^6 \text{ km}^2 \text{ season})^{-1}$ are confined to specific regions. In the spring the maximum is located mainly in the 150°–170°E region, whereas during autumn this threshold is exceeded over a more broadly distributed region across the North Pacific, including a large zone in the Gulf of Alaska. Activity over continental regions is much lower, with mainland Alaska never exhibiting more than 20 storms $(10^6 \text{ km}^2 \text{ season})^{-1}$ in any season, with slightly more activity in autumn and winter.

The Gulf of Alaska emerges as a strong and consistent location for storm lysis and may be considered the ''graveyard of Pacific storms'' (Figs. 5a–d). During winter, lysis density is widespread over the GOA, extending far enough south to present a second maximum over Vancouver Island. Lysis density is lowest in the summer and highest in fall. This could be due to the fact that summer storms last longer and, thus, are able to move farther from the Gulf of Alaska and the North Pacific; as well, the storm count, as reflected by tdens, is lower. Spring and autumn lysis densities exhibit some similar patterns with autumn having slightly larger maxima values. The Bering Sea/Bering Strait areas also present high lysis density, especially in winter and autumn.

Summer storms last longer than winter ones. This is especially true over most of the North Pacific and the

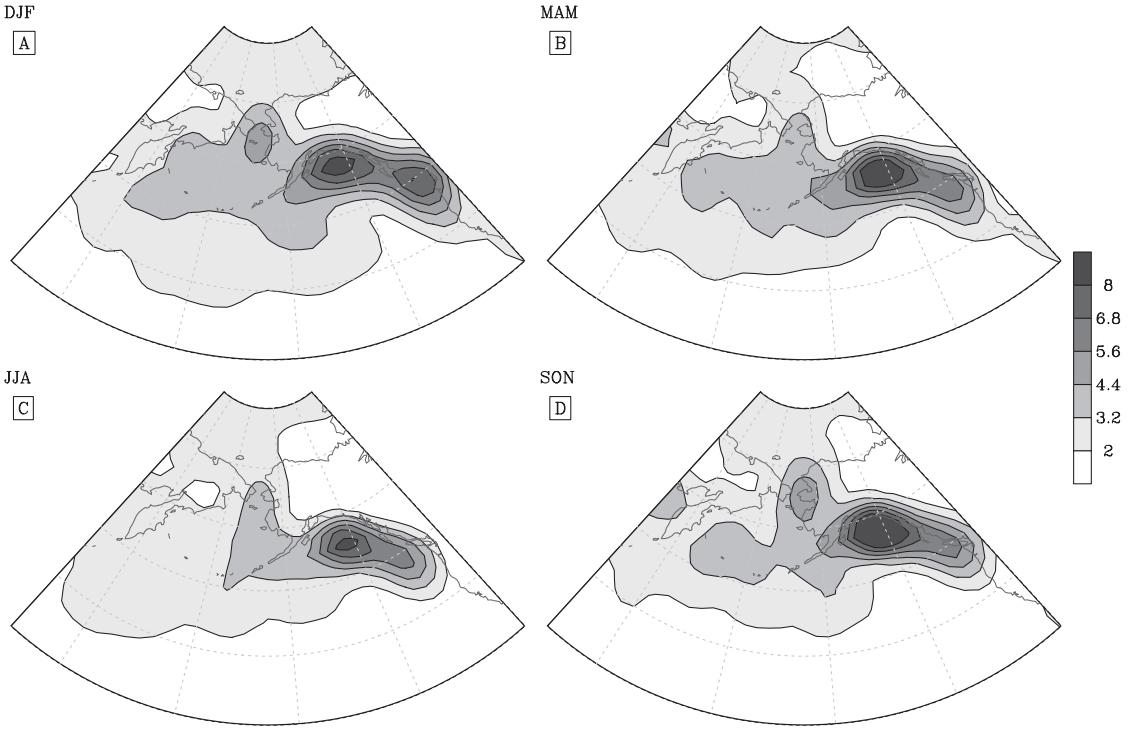

FIG. 5. As in Fig. 3 but for lysis density climatology. Units: density of ending points (10^6 km^2 season)$^{-1}$.

Gulf of Alaska (Figs. 6a–d). Winter storms typically last in excess of 4.5 days over the western North Pacific; spring, storm duration increases to about 5.5 days; and summer storm duration exceeds 5.5 days over most of the North Pacific and the Gulf of Alaska. The large region of Pacific lifetime maxima (>6 days) exhibited in summer is reduced in autumn to a narrower and shorter band extending northeastward to the Aleutian Islands.

The intensity results are based on the filtered vorticity intensities, that is, the T42 intensities with background removed, as discussed in Hoskins and Hodges (2002). Winter storms are most intense (Figs. 7a–d); summer intensities are lowest. Spring and autumn track intensity patterns and magnitudes are quite similar to winter. Winter intensity maxima are situated south of the Bering Sea and Gulf of Alaska. These maxima features are reduced in the other seasons. The summer intensity pattern is also shifted slightly northward and is narrower compared to the other seasons. Unlike the other parameters, for the most part the zone of greatest intensity remains consistently confined to the central Aleutians and to the south.

Storms move most rapidly in winter (Figs. 8a–d), tracking with an average speed of about 14 m s^{-1} over most of the North Pacific, with a maxima west of 160°W along 35°N where the mean track speed exceeds 15.5 m s^{-1}. Spring and autumn patterns are similar to winter, but magnitudes are lower. Summer storms are slowest compared to the other seasons, moving at a typical speed less than 12.5 m s^{-1} over most of the North Pacific, with a maxima core of 11–12.5 m s^{-1} located where the spring and autumn cores are.

b. Trends

In this subsection detailed temporal analyses are presented for three variables: genesis density (gdens), lysis density (ldens), and a new variable defined for this particular assessment: a count of storms that enter the region in question (enter; see Table 1). These are analyzed for the pre- and post-1979 period. Intensity and track density trends are examined using separate plots (Figs. 9–11). Commentary is restricted to significant trends only (above 90% significance levels).

The Alaska interior exhibited six statistically significant trends (Table 1). Two trends were exhibited for the period from 1948/49 to 2008: the spring gdens (+0.93% yr^{-1}) and winter "enter" (−0.44%). The period between 1948/49 and 1978 presented no statistically significant trends. The period from 1979 to 2008 possessed four statistically significant trends: winter gdens (−1.55%), summer gdens (−1.54%), autumn gdens (−1.18%), and the autumn enter (−3.43%).

The Gulf of Alaska exhibited five statistically significant trends for 1948/49–2008 (Table 1), reviewed

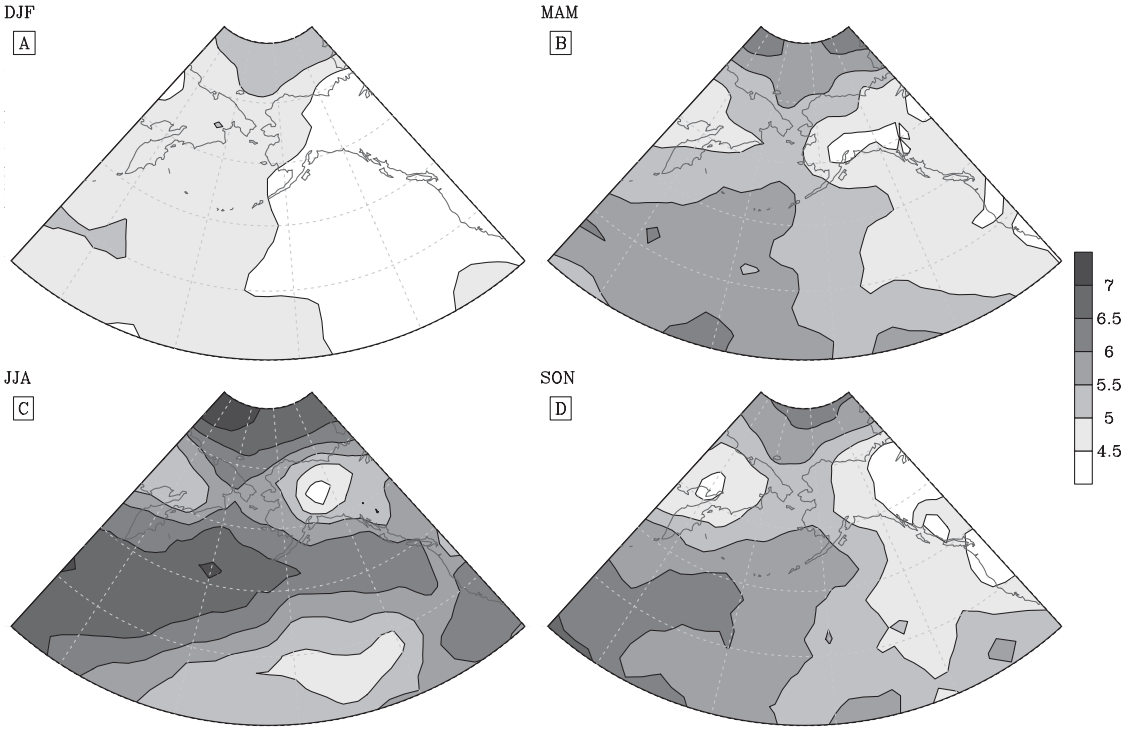

FIG. 6. As in Fig. 3 but for track lifetime climatology. Units: days.

below (rates are percent per year). The gdens exhibited trends in winter (−0.45%) and summer (−0.40%); ldens exhibited trends in winter (+0.55%), spring (+0.59%), and summer (+0.32%). Three trends are significant during the period 1948/49–1978: gdens in winter (−1.15%) and summer (−2.09%) and ldens in summer (+1.08%). One statistically significant trend was apparent for the third period (1979–2008), summer gdens (−1.98%).

Finally, the Bering Sea presented four statistically significant trends: two in the 1948/49–2008 spring ldens (−0.29%) and spring enter (−0.24%). The period from 1948/49 to 1978 shows no statistically significant trends. The period from 1948/49 to 2008 shows two trends: summer ldens (−0.76%) and autumn ldens (+0.79%).

Two other important variables for Alaska are the track density and the track intensity. The track density decadal anomaly patterns show large departures from the mean in the last decade (1999–2008; see Fig. 9). The largest anomalies are observed in these decadal periods: 1949–58, 1979–88, and 1999–2008. Anomalies in the Gulf of Alaska are positive in the last three decadal periods (i.e., since 1979). In the Alaska interior a change in anomaly sign also took place after 1979, represented by an increase from 1979 to 1998 and a decrease in the past decade. As for the Bering Sea, the first two decades show a tdens lower than the mean and the past decades higher.

Intensity (int) is examined using seasonal histograms from 1948/49 to 2008 (Fig. 10). Here, these intensities are the full-resolution intensities obtained by referencing the tracks back to full resolution, computed in the same way as in Bengtsson et al. (2009), by searching for a maximum within a 5° spherical cap region. In the Gulf of Alaska and Bering Sea the most frequently occurring intensity magnitude ranged around 6×10^{-5} s^{-1}, whereas in the Alaska interior intensity magnitudes are lower, ranging around (3–4) $\times 10^{-5}$ s^{-1} for all seasons. In the Gulf of Alaska and Bering Sea the most frequent values shift between 4 and 7 ($\times 10^{-5}$ s^{-1}) in the summer and spring, up to (5–10) $\times 10^{-5}$ s^{-1} in autumn and winter. At the highest end of the scale the Bering Sea has in each season a greater number of higher intensity events than the Gulf of Alaska, including a greater number exceeding 12×10^{-5} s^{-1}. The Alaska interior does not experience such events; maximum intensities are 10×10^{-5} s^{-1}. By season, winter and autumn exhibited the highest number of extreme event cases, commensurate with results already presented. Summer has the fewest number of extreme events and it is the only season in which the histogram of the Gulf of Alaska and the Bering Sea differ the most. The broadest observation from these results is that in every season the Bering Sea has more, higher-intensity events than the Gulf of Alaska.

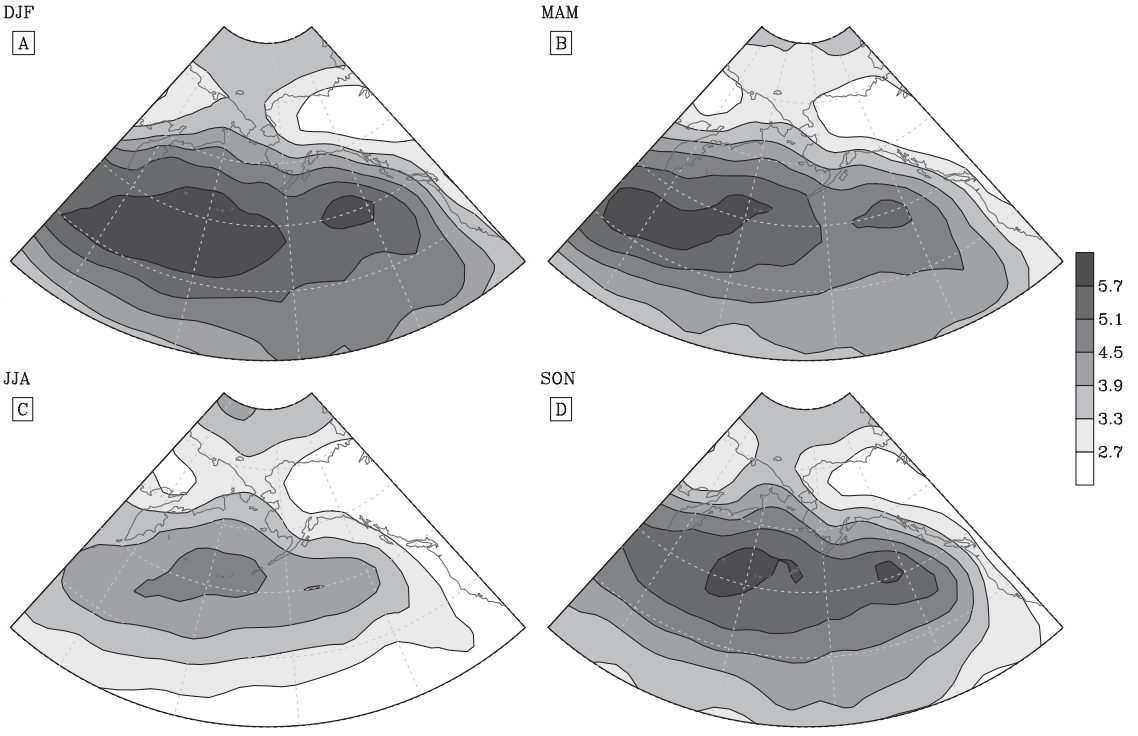

FIG. 7. As in Fig. 3 but for track intensity climatology. Units: 10^{-5} s^{-1}.

A closer look at the winter intensity histogram by decade (Fig. 11) shows that the properties described for Fig. 10 are echoed at this higher temporal resolution. The Alaska interior seems to have had an average of about 1.2–1.6 storms per month for its peak intensity at around 3×10^{-5} s^{-1}. The Gulf of Alaska peak number of events also increased. In the first decades, an average of about 6×10^{-5} s^{-1} was observed. In the past decades, this value has increased to about 9×10^{-5} s^{-1}. The Bering Sea average of 6×10^{-5} s^{-1} for its peak number of events seems to have slightly increased to about 9×10^{-5} s^{-1} until the fourth decade, then decreased in the final two. The histogram changed in the past two decades. The number of extreme events for the Gulf of Alaska and Bering Sea (intensity $>12 \times 10^{-5}$ s^{-1}) increased in the past decade. The Bering Sea had a consistently high number of extreme events through the different decades.

4. Discussion and conclusions

Winter emerged as the most active season for most of the storm parameters, including genesis density and track density. Simmonds and Keay (2002) found high winter mean cyclone occurrences (tdens) over the Sea of Okhotsk and the Gulf of Alaska, which is essentially in accordance with our results, except that we find even higher tdens counts during autumn (a season not considered in their study). Winter storm tracks are also located farther south, a result consistent with many studies (Nakamura 1992; Simmonds and Keay 2002; White 1982). This location is also influenced by the midwinter suppression (Nakamura 1992). One of the key determinants of storm activity is a strong thermal gradient. The north–south gradient of temperature is greatest in the winter. The sea ice extent is farthest south in late winter (Fig. 12). In addition, the Kuroshio Extension (Qiu 2000), also known as the North Pacific Current, acts as a southern anchor for the thermal gradient. The net effect results in a thermal gradient that is strongest in winter. This is conducive to more frequent episodes of baroclinic instability that favor development, growth, and energy levels of extratropical cyclonic systems as is evidenced by descriptions in section 3. An analysis of mean spatial patterns of the index of Eady baroclinic growth rate (not shown) also indicates a maximum zone coincident with fall and winter storms.

The role of diabatic heating is strong in the generation of storms off the east coast of Asia and North America, providing another mechanism for generating the strong thermal gradient mentioned above, which supports the Pacific/Atlantic maxima (Hoskins and Valdes 1990). Release of latent heat also plays an important role in the intensity of the low pressure systems and the rapidity of

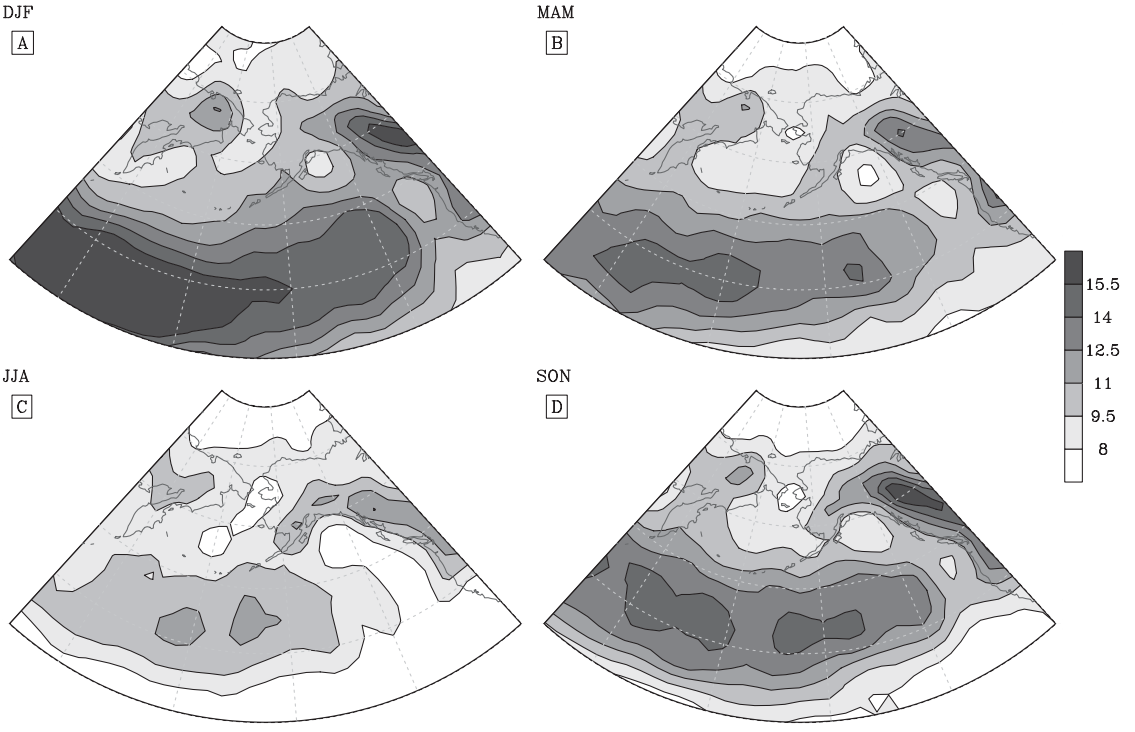

FIG. 8. As in Fig. 3 but for track mean speed climatology. Units: m s^{-1}.

cyclogenesis (Chang et al. 1982; Posselt et al. 2008). In a sense, the NP (and North Atlantic) storm tracks may be considered as self-maintaining, since the diabatic heating maxima in the storm track region are caused by horizontal and vertical flow displacements, which, in turn, are in part a by-product of the individual storms (Hoskins and Valdes 1990). Storm tracks can be self-maintained also by the fact that they help drive the Kuroshio owing to the low-level mean flow induced by the eddy activity and, in turn, the Kuroshio is crucial for the existence of the NP maximum (Hoskins and Valdes 1990).

The lysis density analysis results obtained here reinforces the concept that the Gulf of Alaska is the ''graveyard'' of storms in the NP as pointed out, for example, by Simmonds and Keay (2002). The tdens results (Fig. 4) suggest that most of the storm systems that end up in the Gulf of Alaska do not form locally. A targeted assessment verifies this fact (Fig. 13), which

TABLE 1. Trends of three variables used in this paper: genesis density (gdens), lysis density (ldens) plus an additional metric - the number of storms entering into a region (enter). These trends are divided into periods 1948/49–2008, 1948/49–1978, and 1979–2008 and the three study regions: Alaska interior, Gulf of Alaska, and Bering Sea. Units: % yr^{-1}. Statistically significant values at the 90% significance level italicized, at the 95% significance level underlined and italicized, and at the 99% level in bold. Other values are not statistically significant.

	1948/49–2008				1948/49–1978				1979–2008			
Output variable	DJF	MAM	JJA	SON	DJF	MAM	JJA	SON	DJF	MAM	JJA	SON
Alaska interior												
gdens	0.09	*0.93*	0.46	0.54	−0.46	0.28	−0.27	0.19	*−1.55*	0.49	*−1.54*	**−1.18**
ldens	0.23	0.49	0.61	−0.01	0.66	1.47	1.09	0.69	−1.28	−1.92	−1.13	−1.34
enter	*−0.44*	0.23	−0.17	0.19	−0.18	−0.12	−0.20	1.01	−0.71	1.00	−1.13	−3.43
Gulf of Alaska												
gdens	***−0.45***	−0.14	*−0.40*	−0.27	−1.15	−0.40	**−2.09**	−1.09	−0.86	0.31	**−1.98**	−1.13
ldens	***0.55***	*0.59*	*0.32*	0.22	0.03	1.09	1.08	−0.14	0.63	−0.33	0.95	0.64
enter	0.13	0.08	0.03	0.00	−0.36	−0.47	−0.39	−0.40	0.63	5.34	−0.01	2.91
Bering Sea												
gdens	0.00	−0.34	0.05	−0.01	−0.56	0.22	0.10	−0.49	0.30	0.16	0.19	−0.24
ldens	−0.08	*−0.29*	−0.09	0.06	0.10	0.01	0.05	−0.01	−0.04	0.22	−0.76	0.79
enter	−0.10	*−0.24*	−0.16	−0.11	0.00	−0.10	−0.20	−0.45	0.28	−0.17	−0.61	−0.10

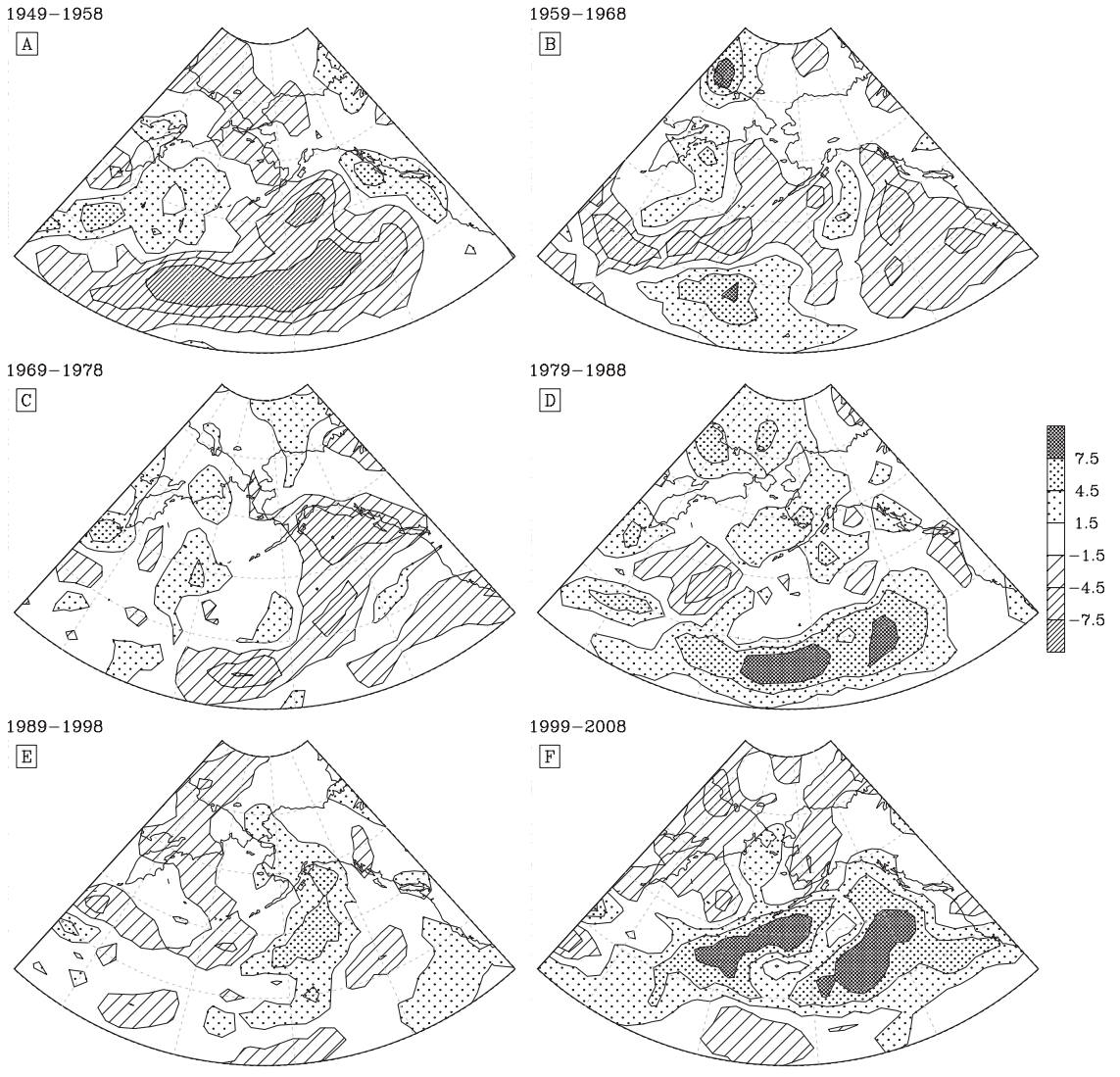

FIG. 9. Track density winter decadal trend represented as the decadal tdens value minus the mean climatology: (a) 1949–58, (b) 1959–68, (c) 1969–78, (d) 1979–88, (e) 1989–98, and (f) 1999–2008.

indicates that most storms are not formed locally, with the exception of the summer season, for which a source region in the Aleutian Islands is indicated. Also, the midocean cyclogenesis is likely due to secondary cyclogenesis and downstream development, as discussed in Hoskins and Hodges (2002). This may also be roughly concluded by realizing that the mean track speed (12 m s^{-1}) and lifetime (5 days) of these storms (winter considered) results in a lifetime distance traveled of ~5000 km. Another important aspect is the fact that there are indications of tropical cyclones undergoing extratropical transitions and reaching GOA, especially during summer and autumn (Fig. 14).

Once in the Gulf of Alaska, there are several mechanisms at work that contribute to the large observed lysis values. First, barotropic processes typically are the dominant dynamical mechanisms at work. Understanding the role played by barotropic processes is important since the life cycles of baroclinic waves in a zonally symmetric flow are characterized by positive conversions in the growth phase and negative barotropic conversions in the decay phase (Frisius et al. 1998; Simmons and Hoskins 1978). This way, barotropic processes play an important role in the lysis phase of the storm tracks. Second, and perhaps exerting greater importance, the role of regional topography must be considered. The topography of coastal Alaska and northwest North America—the coastal highlands and mountains—is manifested as an influencing agent because its physical presence could be great enough to help destroy shear.

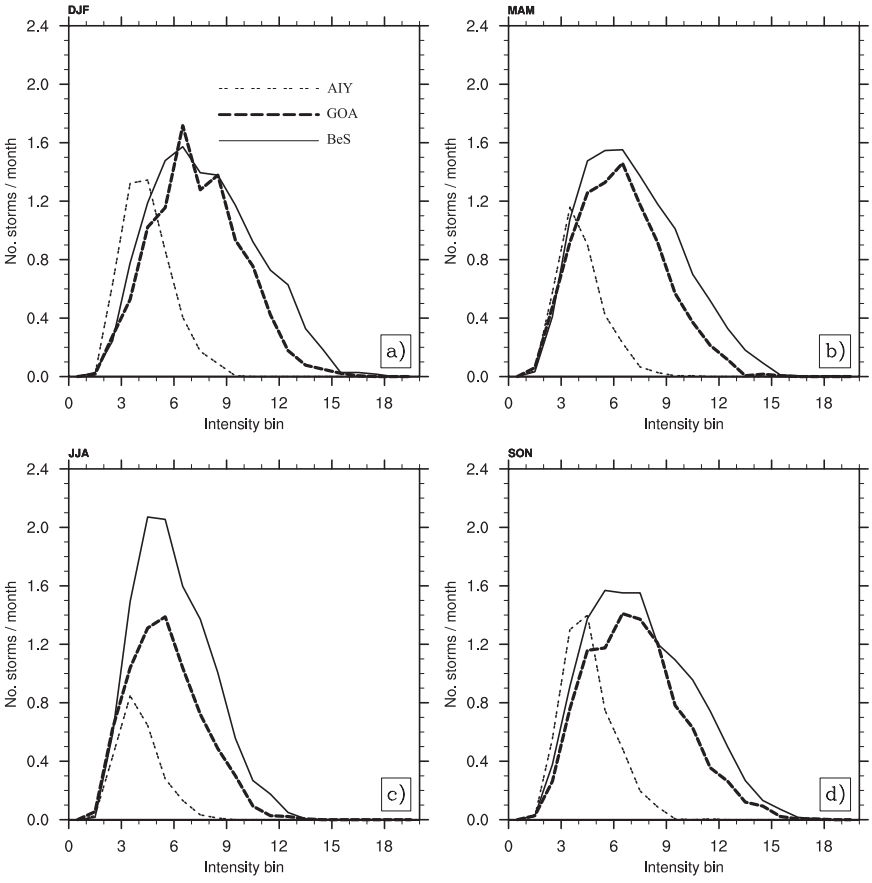

FIG. 10. Intensity distributions calculated from the full-resolution data for AIY, GOA, and BeS from 1948/49 to 2008: (a) DJF, (b) MAM, (c) JJA, and (d) SON. Intensity is in units of 10^{-5} s^{-1}; bin width is 1×10^{-5} s^{-1}.

The shear of the meridional wind and the zonal wind contribute equally to the total shear production (destruction) (Frisius et al. 1998). Negative shear production has been shown to be responsible for the location of the ''downstream end'' of the storm track (Frisius et al. 1998; Whitaker and Dole 1995). Shear destruction of the transient eddies (barotropic processes) associated with lysis reduces the turbulent kinetic energy (TKE) because via this process, eddies release kinetic energy to the mean flow [TKE = advection + baroclinic production + shear production (destruction) + dissipation] and the storms die out, in this case, in the Gulf of Alaska (Black and Dole 2000; Frisius et al. 1998).

Another factor at work in the NP context is the presence of a favored location for a downstream blocking ridge over the Aleutians/Alaska region, also known as the ''Alaska block'' pattern (Frisius et al. 1998; Lau 1988), which can act to retard the eastward progression of systems along the Pacific storm track. According to Simmonds and Keay (2002), the Gulf of Alaska is also a region of high cyclone frequency; however, this is not incompatible with high lysis values because GOA is also an area of strong baroclinicity, indicated by the Eady growth rate assessment, which can enhance activity, and because systems can become stalled against topography or blocking patterns, mentioned above, which could enhance residence time. Thus, both the barotropic deformation (D) and the tropospheric baroclinic growth (B) could play an important role in the dynamics over the Gulf of Alaska, as illustrated by the ratio of D/B over GOA, as shown by Black and Dole (2000). Such a result is consistent with a relatively high Eady growth rate, an indicator that is proportional to vertical shear.

As for the lifetime, summer storms last longer than any other season. This result expands upon two previous studies (Mesquita et al. 2008; Zhang et al. 2004) that confined comparisons of lifetime to summer and winter. Summer storms are also the least intense with winter, spring, and autumn intensities being greater and similar to one another. Simmonds and Keay (2002) also found that, in general, the mean intensity is significantly reduced in summer with the most intense summer systems

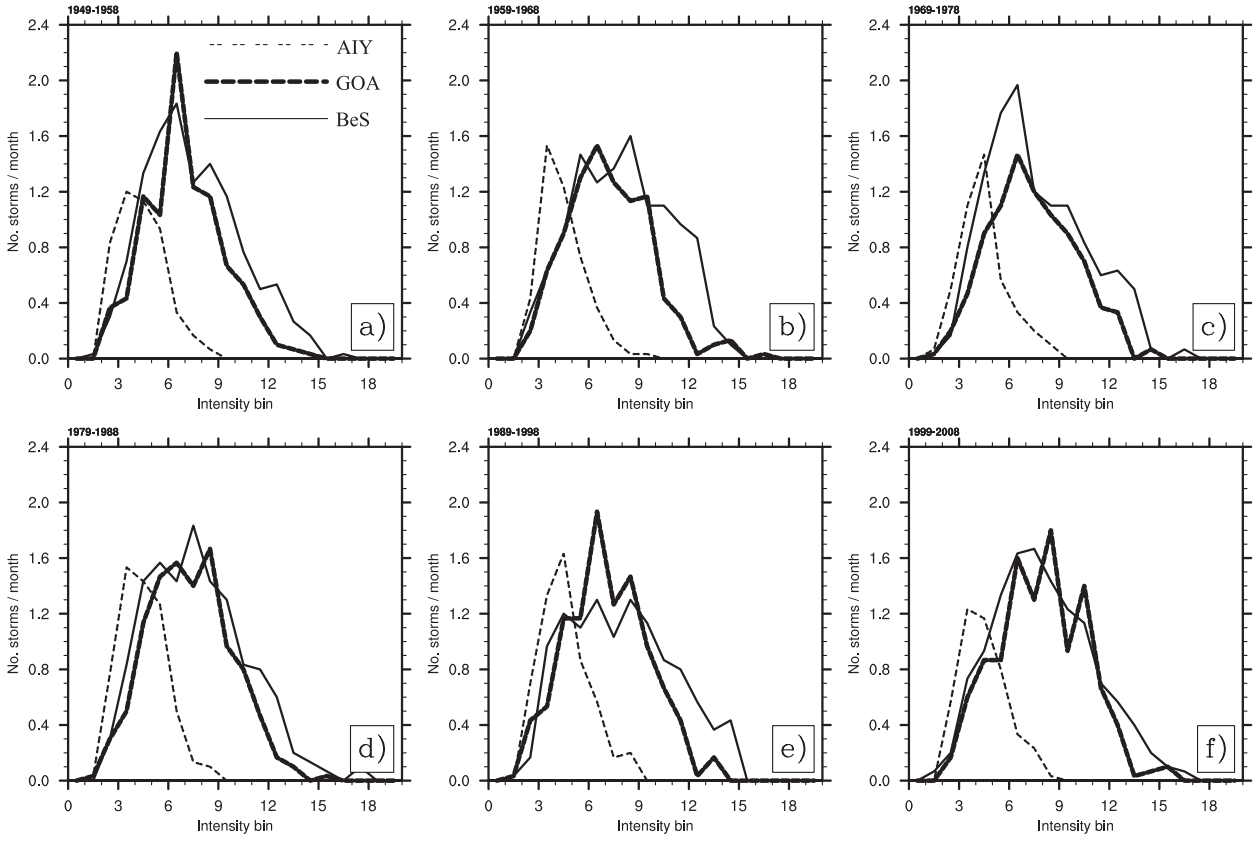

FIG. 11. The decadal DJF intensity distributions calculated from the full-resolution data for AIY, GOA, and BeS: (a) 1949–58, (b) 1959–68, (c) 1969–78, (d) 1979–88, (e) 1989–98, and (f) 1999–2008. Intensity is in units of 10^{-5} s^{-1}; bin width is 1×10^{-5} s^{-1}.

found over and southwest of the Aleutian region, also in accordance with our results. Their intensity plots, using a different measure of intensity, of the winter and summer intensity resemble our intensity DJF and JJA plots as well. Finally, the mean speed of the storms is higher in winter. In summary, summer storms last longer, move more slowly, and are less intense. A common factor linking these traits together is the growth rate (not shown). Summer storms tend to have much lower growth rates. One import feature of the climatology analysis is that the transitional seasons, spring and autumn, tended to have similar values for most of the storm parameters considered.

Whitaker and Dole (1995) mention that storm tracks exhibit considerable variability in interannual and intraseasonal time scales. We agree that interannual variability is considerable and are able to shed more light on the interseasonal issue; however, we have found a different result in our study concerning the interseasonal aspect: spring and autumn present similar characteristics for all of the variables with the exception that autumn intensity is stronger than in spring. Small differences in lifetime and lysis were also noted (autumn was larger in both cases). The greatest contrasts are observed during winter and summer, which are the times of greatest contrasts in temperature gradients. Summer storms have the lowest values for genesis, track density, intensity, and lysis. Summer storms, however, last longer than winter ones. This is in accordance with Zhang et al. (2004) and Mesquita et al. (2008). This result is expanded here to show that they last longer than in any of the other seasons. The track density (tdens) results by decade (Fig. 9) underscore the strong interannual and interdecadal variability that work against isolation of a trend signal.

Maxima spatial patterns exhibited a north/south shift. The main factor responsible for the maintenance of this zonal variation of baroclinicity is the distribution of heating (Frisius et al. 1998; Hoskins and Valdes 1990). A rotation ''point'' in the central Aleutian Islands as, for example, in the gdens, tdens, and mspd cases, was also apparent. This dogleg in the storm tracks observed here is caused in part by the temperature gradient changes in the North Pacific, but is also suspected to be a by-product of a midtropospheric (700 mb) moisture pattern in which the Bering Sea region is drier than the Gulf of Alaska in all seasons except summer (not shown).

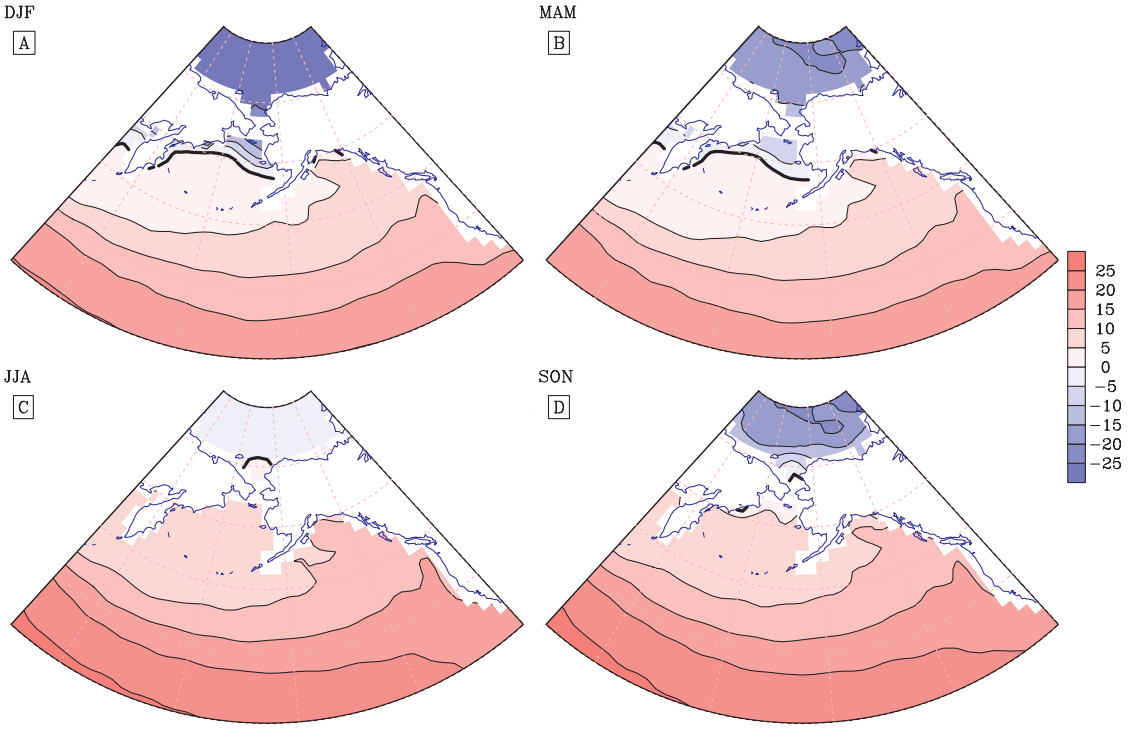

FIG. 12. Mean SST (°C) in the North Pacific from 1948/49 to 2008 from NCEP–NCAR Reanalysis for (a) winter (DJF), (b) spring (MAM), (c) summer (JJA), and (d) autumn (SON). The thick line represents the 0°C isotherm, which provides a functional indication of the average sea ice extent.

Of the three aggregate regions considered in this paper, AIY has higher annual genesis compared to the other regions, GOA has a higher number of storms (tdens) and higher lysis, and BeS shows storms with longer lifetime and greater intensity, and speed. When considering storms with intensities exceeding 12×10^{-5} s^{-1}, however, BeS was found to consistently possess more of these strong intensity storms than GOA (Fig. 10). The Eady growth rate analysis indicated a zone of high Eady potential south of Russia's Kamchatka Peninsula, which can serve to reenergize older systems as they move into BeS. It is hypothesized here that, by the time systems enter GOA, the increasing shear regime coupled with greater downstream distance from the Kamchatka Eady max precludes stronger development in most cases.

In general, most of the storm parameters trends observed in this study were not very robust. Most of the statistically significant trends at the 99% significance level are related to the genesis for the AIY region and genesis and lysis for BeS. The fact that different trends are found for the periods before and after 1979 reflects an underlying factor in this case: the influence of large modes of climatic variability, which may play an important role in such trends. These issues are considered in a companion paper. The issue of fleeting statistical significance speaks to both a few degrees of freedom issue caused by the relatively short time series available to work with and the large interannual variability observed in these variables. A possible additional source of pre- and post-1979 variability could be due to the introduction of large quantities of satellite data into the reanalysis after 1979, which has progressively increased with time (Bengtsson et al. 2004; Bromwich et al. 2007). There are a variety of points to make about the trends results, however.

When considering the trends for the three regions and the three different periods of time—the entire 1948–2008 time series and pre- and post-1979—we observe that most of the trends that are statistically significant (at the 95% and 99% significance levels) occur in the GOA region, generally for genesis density and lysis density. An interesting point is that Latif and Barnett (1996) showed strong positive SST trends for GOA. Positive SST trends and SST gradients are also observed in the NCEP–NCAR reanalysis data (not shown). Despite this, strong positive trends are not noted for those storm parameters that would be influenced by SST forcing, namely, genesis density: gdens decreases wherever its trend is significant. Hence, SST does not appear to be a key storm-forcing agent in the Gulf of Alaska. Some

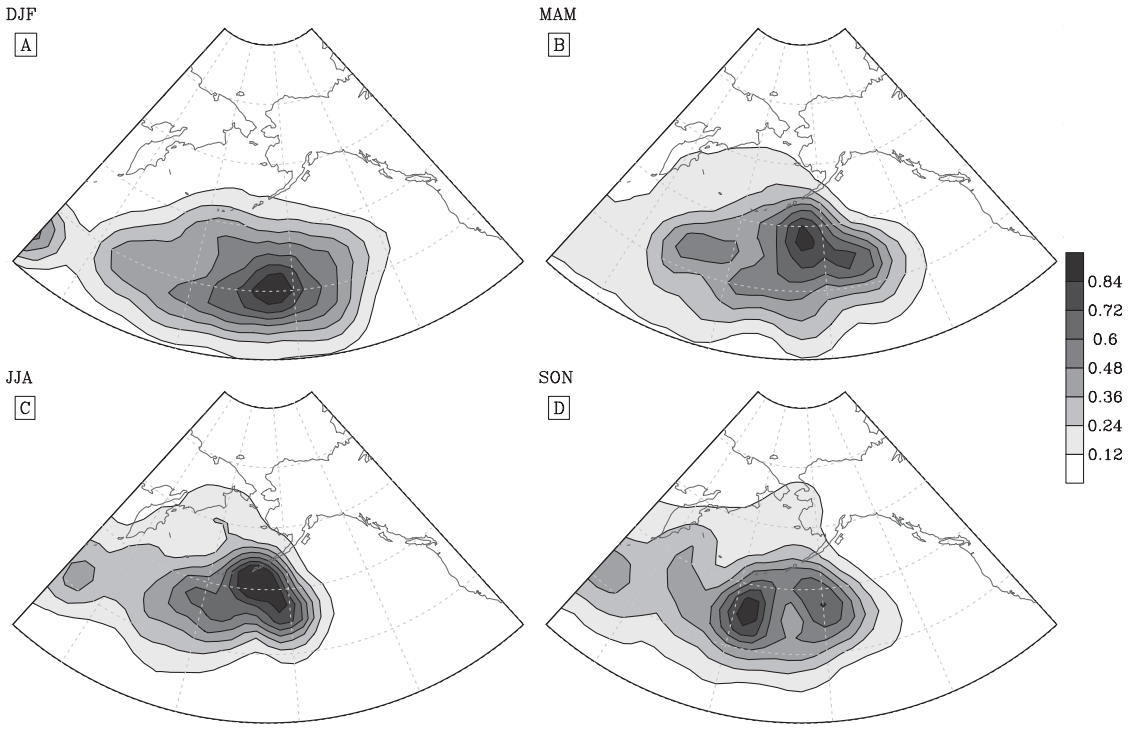

FIG. 13. Contour plots of the genesis density variable for all storms possessing end-points in the Gulf of Alaska study zone: sampling region within a 5° spherical cap centered at 56°N, 147°W; timeframe is the entire 1948/49–2008 study period; plots are broken down seasonally as (a) DJF, (b) MAM, (c) JJA, and (d) SON. Units: density of starting points $(10^6 \text{ km}^2 \text{ season})^{-1}$.

studies have related the sea ice cover in the Sea of Okhotsk to the location and intensity of the Aleutian low, which could play an important role in the GOA trends. For example, Honda et al. (1999) suggest a significant influence of ice cover on the downstream pressure field. Few strong, significant trends were noted for the Alaska interior. As for the Bering Sea, not many trends were found there.

Two variables are of particular importance for Alaska when it concerns trends: the number of storms (tdens or enter) and their intensity (int). None of the three regions considered show significant trends for these variables. Other studies have suggested that ''storms are increasing.'' For example, McCabe et al. (2001), using Serreze's (1995) tracking algorithm, found a considerable increase in cyclone frequency in high latitudes (60°–90°N) and a pronounced decrease in midlatitudes (30°–60°N). The results of McCabe et al. represented broadly integrated swaths. Our results, however, indicate that, for the regions considered here, this is not really the case: there is no particular trend in storm activity in the AIY, BeS, or GOA regions.

As for the intensity, this result also appears to contrast with the paper by McCabe et al. (2001), who found that the storm intensity has increased both in mid and high latitudes. Graham and Diaz (2001) found an intensification of NP winter cyclones, which resulted from the increasing upper-tropospheric zonal winds between 25° and 40°N associated with ENSO. It is not simple to compare trends in intensity with McCabe et al. (2001) and Graham and Diaz (2001) because of the different approaches used to define and calculate the intensity variable. This could also be due to the use of pressure, which can be influenced by the large-scale background. If intensity is measured as the pressure minima, as in Graham and Diaz (2001), it would be influenced by any large-scale changes. However, the lack of intensity trends found in our study is consistent with the fact that these regions are a little north of the main path/track of the Pacific maximum, except the GOA, which is the region with high lysis density.

An interesting result is a clear indication that SST does not appear to be a strong storm control for the marine regions explicitly considered: the Gulf of Alaska and Bering Sea. Instead, local shear and topography conditions appear to exert the greater control. This is important in light of potential future increasing trends in SST if sea ice continues to retreat, that is, that storm activity will not follow suit because of SST alone. It is important to note that, overall, Bering Sea trends are

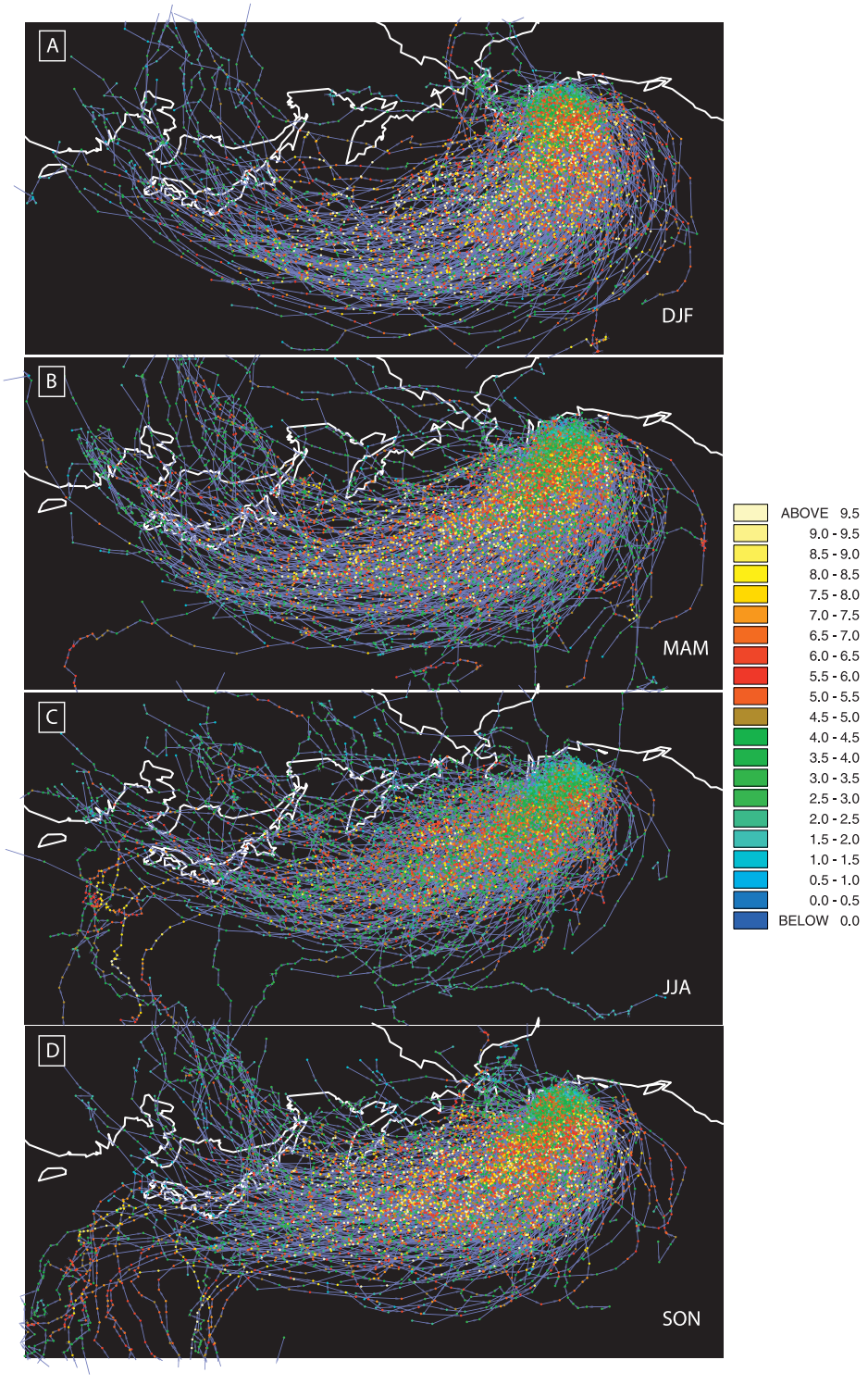

FIG. 14. Plots of all storms possessing endpoints in the Gulf of Alaska study zone. Timeframe is the entire 1948/49–2008 study period; plots are broken down seasonally as (a) DJF, (b) MAM, (c) JJA, and (d) SON. The color scheme represents the T42 intensities with background removed, with units of 10^{-5} s^{-1}.

difficult to identify in part because of high interannual variability. The relative lack of influence of SST also shows up in the lysis values that remain relatively consistent all along the west coast, even in the presence of considerable SST gradients.

Acknowledgments. This research was funded by the National Oceanic and Atmospheric Administration (NOAA) under the project title ''Social vulnerability to climate change in the Alaskan coastal zone'' (Grant NA06OAR4600179). We are grateful for NCAR for providing their datasets in the public domain. We would like to thank Dr. John Walsh, from the International Arctic Research Center at the University of Alaska Fairbanks, for the invaluable comments on the paper. We also thank Dr. Asgeir Sorteberg, from the University of Bergen (Norway), and Christine Radermacher, from the University of Bonn (Germany), for the initial data setup discussions. We appreciate comments made by the anonymous reviewers.

REFERENCES

Atkinson, D. E., 2005: Observed storminess patterns and trends in the circum-Arctic coastal regime. *Geo-Mar. Lett.,* **25** (2–3), 98–109.

Barry, R. G., and A. M. Carleton, 2001: *Synoptic and Dynamic Climatology*. Routledge, 620 pp.

Bell, G. D., and L. F. Bosart, 1989: A 15-year climatology of Northern Hemisphere 500 mb closed cyclone and anticyclone centers. *Mon. Wea. Rev.,* **117,** 2142–2164.

Bengtsson, L., S. Hagemann, and K. I. Hodges, 2004: Can climate trends be calculated from reanalysis data? *J. Geophys. Res.,* **109,** D11111, doi:10.1029/2004JD004536.

——, K. I. Hodges, and N. Keenlyside, 2009: Will extratropical storms intensify in a warmer climate? *J. Climate,* **22,** 2276–2301.

Black, R. X., and R. M. Dole, 2000: Storm tracks and barotropic deformation in climate models. *J. Climate,* **13,** 2712–2728.

Bromwich, D. H., R. L. Fogt, K. I. Hodges, and J. E. Walsh, 2007: A tropospheric assessment of the ERA-40, NCEP, and JRA-25 global reanalyses in the polar regions. *J. Geophys. Res.,* **112,** D10111, doi:10.1029/2006JD007859.

Chang, C. B., D. J. Perkey, and C. W. Kreitzberg, 1982: A numerical case study of the effects of latent heating on a developing wave cyclone. *J. Atmos. Sci.,* **39,** 1555–1570.

Frisius, T., F. Lunkeit, K. Fraedrich, and I. N. James, 1998: Storm-track organization and variability in a simplified atmospheric global circulation model. *Quart. J. Roy. Meteor. Soc.,* **124,** 1019–1043.

Graham, N. E., and H. F. Diaz, 2001: Evidence for intensification of North Pacific winter cyclones since 1948. *Bull. Amer. Meteor. Soc.,* **82,** 1869–1893.

Hodges, K. I., 1994: A general method for tracking analysis and its application to meteorological data. *Mon. Wea. Rev.,* **122,** 2573–2586.

——, 1995: Feature tracking on the unit sphere. *Mon. Wea. Rev.,* **123,** 3458–3465.

——, 1996: Spherical nonparametric estimators applied to the UGAMP model integration for AMIP. *Mon. Wea. Rev.,* **124,** 2914–2932.

——, 1999: Adaptive constraints for feature tracking. *Mon. Wea. Rev.,* **127,** 1362–1373.

——, B. J. Hoskins, J. Boyle, and C. Thorncroft, 2003: A comparison of recent reanalysis datasets using objective feature tracking: Storm tracks and tropical easterly waves. *Mon. Wea. Rev.,* **131,** 2012–2037.

Holton, J. R., 2004: *An Introduction to Dynamic Meteorology*. 4 ed. Elsevier, 535 pp.

Honda, M., K. Yamazaki, H. Nakamura, and K. Takeuchi, 1999: Dynamic and thermodynamic characteristics of atmospheric response to anomalous sea-ice extent in the Sea of Okhotsk. *J. Climate,* **12,** 3347–3358.

Hoskins, B. J., and P. J. Valdes, 1990: On the existence of storm tracks. *J. Atmos. Sci.,* **47,** 1854–1864.

——, and K. I. Hodges, 2002: New perspectives on the Northern Hemisphere winter storm tracks. *J. Atmos. Sci.,* **59,** 1041–1061.

Kalnay, E., and Coauthors, 1996: The NCEP/NCAR 40-Year Reanalysis Project. *Bull. Amer. Meteor. Soc.,* **77,** 437–471.

Keegan, T. J., 1958: Arctic synoptic activity in winter. *J. Atmos. Sci.,* **15,** 513–521.

Key, J. R., and A. C. K. Chan, 1999: Multidecadal global and regional trends in 1000 mb and 500 mb cyclone frequencies. *Geophys. Res. Lett.,* **26,** 2053–2056.

Kistler, R., and Coauthors, 2001: The NCEP–NCAR 50-Year Reanalysis: Monthly means CD-ROM and documentation. *Bull. Amer. Meteor. Soc.,* **82,** 247–267.

Latif, M., and T. P. Barnett, 1996: Decadal climate variability over the North Pacific and North America: Dynamics and predictability. *J. Climate,* **9,** 2407–2423.

Lau, N.-C., 1988: Variability of the observed midlatitude storm tracks in relation to low-frequency changes in the circulation pattern. *J. Atmos. Sci.,* **45,** 2718–2743.

McCabe, G. J., M. P. Clark, and M. C. Serreze, 2001: Trends in Northern Hemisphere surface cyclone frequency and intensity. *J. Climate,* **14,** 2763–2768.

Mesquita, M. d. S., N. G. Kvamstø, A. Sorteberg, and D. E. Atkinson, 2008: Climatological properties of summertime extra-tropical storm tracks in the Northern Hemisphere. *Tellus,* **60A,** 557–569.

Murray, R., and I. Simmonds, 1991: A numerical scheme for tracking cyclone centres from digital data. Part I: Development and operation of the scheme. *Aust. Meteor. Mag.,* **39,** 155–166.

Nakamura, H., 1992: Midwinter suppression of baroclinic wave activity in the Pacific. *J. Atmos. Sci.,* **49,** 1629–1642.

Norris, J. R., 2000: Interannual and interdecadal variability in the storm track, cloudiness, and sea surface temperature over the summertime North Pacific. *J. Climate,* **13,** 422–430.

Pickart, R. S., G. W. K. Moore, A. M. Macdonald, I. A. Renfrew, J. E. Walsh, and W. S. Kessler, 2009: Seasonal evolution of Aleutian low-pressure systems: Implications for the North Pacific sub-polar circulation. *J. Phys. Oceanogr.,* **39,** 1317–1339.

Posselt, D. J., G. L. Stephens, and M. Miller, 2008: CLOUDSAT: Adding a new dimension to a classical view of extratropical cyclones. *Bull. Amer. Meteor. Soc.,* **89,** 599–609.

Qiu, B., 2000: Interannual variability of the Kuroshio Extension system and its impact on the wintertime SST field. *J. Phys. Oceanogr.,* **30,** 1486–1502.

Rachold, V., F. E. Are, D. E. Atkinson, G. Cherkashov, and S. M. Solomon, 2005: Arctic coastal dynamics—An introduction. *Geo-Mar. Lett.,* **25** (2–3), 63–68.

Serreze, M. C., 1995: Climatological aspects of cyclone development and decay in the Arctic. *Atmos.–Ocean,* **33,** 1–23.

——, F. Carse, R. G. Barry, and J. C. Rogers, 1997: Icelandic low cyclone activity: Climatological features, linkages with the NAO, and relationships with recent changes in the Northern Hemisphere circulation. *J. Climate,* **10,** 453–464.

——, A. H. Lynch, and M. P. Clark, 2001: The Arctic frontal zone as seen in the NCEP–NCAR reanalysis. *J. Climate,* **14,** 1550–1567.

Simmonds, I., and K. Keay, 2002: Surface fluxes of momentum and mechanical energy over the North Pacific and North Atlantic Oceans. *Meteor. Atmos. Phys.,* **80,** 1–18.

Simmons, A. J., and B. J. Hoskins, 1978: The life cycles of some nonlinear baroclinic waves. *J. Atmos. Sci.,* **35,** 414–432.

Sinclair, M. R., 1994: An objective cyclone climatology for the Southern Hemisphere. *Mon. Wea. Rev.,* **122,** 2239–2256.

Sorteberg, A., and J. E. Walsh, 2008: Seasonal cyclone variability at 70°N and its impact on moisture transport into the Arctic. *Tellus,* **60A,** 570–586.

Twitchel, P. F., E. A. Rasmussen, and K. L. Davidson, 1989: *Polar and Arctic Lows*. A. Deepak, 421 pp.

Whitaker, J. S., and R. M. Dole, 1995: Organization of storm tracks in zonally varying flows. *J. Atmos. Sci.,* **52,** 1178–1191.

White, G. H., 1982: An observational study of the Northern Hemisphere extratropical summertime general circulation. *J. Atmos. Sci.,* **39,** 24–40.

Whittaker, L., and L. Horn, 1984: Northern Hemisphere extratropical cyclone activity for four mid-season months. *J. Climatol.,* **4,** 297–310.

Zhang, X., J. E. Walsh, J. Zhang, U. S. Bhatt, and M. Ikeda, 2004: Climatology and interannual variability of Arctic cyclone activity: 1948–2002. *J. Climate,* **17,** 2300–2317.